Hydrol. Earth Syst. Sci. Discuss., https://doi.org/10.5194/hess-2018-232
Manuscript under review for journal Hydrol. Earth Syst. Sci.
Discussion started: 14 May 2018

Hydrology and Earth System Sciences
Open Access
Discussions

Quantifying projected changes in runoff variability and flow regimes of the Fraser River Basin, British Columbia

Siraj Ul Islam[1*], Charles L. Curry[2], Stephen J. Déry[1], and Francis W. Zwiers[2]

[1]Environmental Science and Engineering Program,
University of Northern British Columbia, Prince George, British Columbia (BC), V2N 4Z9, Canada

[2]Pacific Climate Impacts Consortium,
University of Victoria, Victoria, BC, V8W 2Y2, Canada

Correspondence to: Siraj Ul Islam (sirajul.islam@unbc.ca)

Abstract. Canada's Fraser River Basin (FRB), the largest watershed in the province of British Columbia, supplies vital freshwater resources and is the world's most productive salmon river system. We evaluate projected changes in the FRB's runoff variability and regime transitions using the Variable Infiltration Capacity (VIC) hydrological model. The VIC model is driven by an ensemble of 21 statistically downscaled simulations from the Coupled Model Intercomparison Project Phase 5 (CMIP5), for a 150-year time period (1950-2099) over which greenhouse gas concentrations follow the CMIP5 Representative Concentration Pathway (RCP) 8.5. Using mean and standard deviation (variability) metrics, we emphasize projected hydroclimatological changes in the cold season (October to March) over different sub-basins and geoclimatic regions of the FRB.

Warming consistent with the RCP8.5 scenario would lead to increased precipitation input to the basin with higher interannual variability and considerably reduced winter snowfall shortening the average snow accumulation season by about 38%. Such changes in temperature and precipitation will increase cold season runoff variability leading to higher cold season peak flows. In the lower Fraser River, cold season runoff will increase by 70% and its interannual variability will double compared to

Hydrol. Earth Syst. Sci. Discuss., https://doi.org/10.5194/hess-2018-232
Manuscript under review for journal Hydrol. Earth Syst. Sci.
Discussion started: 14 May 2018

the 1990s, presenting substantial challenges for operational flow forecasting by the end of this century. Cold season peak flows will increase substantially, particularly in the Coast Mountains, where the peak flow magnitudes will rise by 60%. These projected changes are consistent with a basin-wide transition from a snow-melt driven flow regime to one that more closely resembles a rainfall driven regime. This study provides key information relating to projected hydroclimate variability across the FRB, describes potential impacts on its water resources, and assesses the implications for future extreme hydrological events.

Keywords: Climate change, hydrological modelling, runoff, snow, Fraser River

Hydrol. Earth Syst. Sci. Discuss., https://doi.org/10.5194/hess-2018-232
Manuscript under review for journal Hydrol. Earth Syst. Sci.
Discussion started: 14 May 2018

1 Introduction

The Fraser River Basin (FRB) is one of the largest watersheds draining the western Cordillera of North America (Benke and Cushing, 2005). It spans 240,000 km^2 of diverse landscapes including dry interior plateaus bounded by the Rocky Mountains to the east and the Coast Mountains to the west. Its elevation ranges from sea level to 3954 m at its tallest peak, Mt. Robson in the Rocky Mountains (Benke and Cushing, 2005). Descending at Fraser Pass near Blackrock Mountain, the Fraser River runs 1400 km before draining into the Strait of Georgia and Salish Sea at Vancouver, British Columbia (BC) (Schnorbus et al., 2010). The FRB's rich diversity and abundance of natural resources yield economic opportunities and prosperity related to agriculture, fishing, forestry, mining, hydropower production, tourism and recreation (Benke and Cushing, 2005). As an extensive freshwater aquatic ecosystem, it remains the most important salmonid-producing river system in North America, sustaining the largest migrations of Pacific Ocean sockeye salmon in the world (Labelle, 2009; Eliason et al., 2011). The Fraser River also forms the aquatic habitat of North America's largest wild population of white sturgeon now listed as an endangered species due to its declining populations (Scott and Crossman, 1973; McAdam et al., 2005; Hildebrand et al., 2016).

Over the past 60 years, mean annual surface air temperature in the FRB has risen by 1.4°C modifying the FRB's natural water cycle (Kang et al., 2014). Impacts of this warming include reductions in snow accumulations (Danard and Murty, 1994), decline in the contribution of snow to runoff generation (Kang et al., 2014) and earlier melt-driven runoff with subsequent reductions in summer flows (Kang et al., 2016). The corresponding changes in mean flow (Danard and Murty, 1994; Morrison et al., 2002; Ferrari et al., 2007; Kang et al., 2014, 2016) have been accompanied by

Hydrol. Earth Syst. Sci. Discuss., https://doi.org/10.5194/hess-2018-232
Manuscript under review for journal Hydrol. Earth Syst. Sci.
Discussion started: 14 May 2018

considerable amplification in the interannual variability of the flow over recent decades across many streams and rivers in the FRB (Déry et al., 2012).

In general, the dominant climatic drivers of water availability are precipitation, temperature, and evapotranspiration with the relative importance of each varying by geographic location. Projected warming will likely result in considerable changes in mean evapotranspiration and precipitation (Collins et al., 2013). Along with mean precipitation, its variability is also expected to increase on daily to interannual timescales over almost all global land areas in response to global warming (Pendergrass et al., 2017). In the FRB, further warming will continue to modify the partitioning of precipitation phase, decreasing the overall snow-to-rain ratio (Islam et al., 2017). Such changes, along with expected increases in precipitation variability, will alter the magnitude and timing of seasonal flows in the FRB and increase the potential for flooding (Curry et al., 2018, in preparation), thus threatening the natural, ecological and social systems within the basin.

Shrestha et al. (2012), Kang et al. (2014, 2016), and Islam et al. (2017) have evaluated observed and projected changes in the timing and magnitude of summer runoff focusing on FRB mean climatological hydrographs. In contrast, little attention has been focused on the detection of changes in flow variability. It is crucial to quantify projected changes in FRB runoff variability on daily and interannual timescales induced by changes in the proportionality of snowfall to rainfall and snowmelt-driven runoff timing. Furthermore, rising air temperatures and precipitation changes, and resulting runoff changes, will also modify the characteristics of FRB flow regimes. Currently, the hydrologic response in the FRB varies considerably across the basin due to its complex topography and maritime influences that differentiate its flows mainly into snow-dominant or hybrid (rain and snow) regimes (Wade et al., 2001). Under future climatic perturbations, these distinct flow regimes could be expected to change, with hybrid or rainfall-dominant flow regimes becoming more prevalent. It is important to evaluate such regime transitions on regional scales while characterizing snowmelt and rainfall driven flows independently.

The principal goals of this study are therefore to investigate how projected climatic change could lead to changes in the mean state and variability of FRB flows, and to evaluate the likelihood of transitions from snowmelt-dominant to hybrid snowmelt-rainfall or rainfall-dominant flow regimes. By extension, this will provide new information about possible changes in extreme events such as flooding. Our approach consists of conducting a systematic investigation of FRB flows by evaluating how projected changes in snow hydrology will impact: i) runoff variability and intensity on daily and interannual timescales, and; ii) flow regimes driven by annual snowmelt freshets. We utilize a semi-distributed, macroscale hydrological model driven by 21 downscaled simulations of future climate from Global Climate Models (GCMs). An important aspect of this study involves the use of a snowmelt pulse detection technique to evaluate transitions between distinct runoff regimes. This approach provides insight into the location and timing of these transitions, while the use of many different GCM-driven hydrological simulations allows a concomitant estimate of the associated uncertainties.

2. Domain, Modelling Framework, and Methodology

2.1 Study domain

Our primary focus was on the Fraser River main stem at Hope, BC (Lower Fraser, LF) since it integrates flows from about 94% of the FRB, and is the location of the longest instrumental streamflow record for the basin's main stem. We also considered four mountainous sub-basins (the Upper Fraser (UF), Quesnel (QU), Chilko (CH) and Thompson-Nicola (TN) Rivers; Fig. 1a, Table 1), along with three geo-climatic regions within the FRB (the Interior Plateau, the Rocky Mountains, and the Coast Mountains; Moore, 1991, Fig. 1b). The FRB exhibits snowmelt-dominant flows in the Interior Plateau and Rocky Mountains in late spring and early summer. However, several catchments in the Coast Mountains and in the Lower Mainland exhibit a secondary runoff peak owing to Pacific frontal rainstorms often associated with atmospheric rivers in October-December. Together, these regions represent the range of distinctive physiographic and hydro-climatic conditions found within the FRB.

2.2 Climate Models, Observational Data, and Statistical Downscaling

We used statistically downscaled climate simulations from 21 GCMs (Supplementary Table 1) submitted to the Coupled Models Intercomparison Project Phase 5 (CMIP5) (Taylor et al., 2012). A single realization was used from each GCM, driven by historical greenhouse gas and aerosol forcing up to 2005 and Representative Concentration Pathway 8.5 (RCP 8.5) forcing subsequently. GCM simulated daily precipitation and daily maximum and minimum surface air temperature for the period 1950-2099, downscaled to 10-km spatial resolution, were obtained from the Pacific Climate Impacts Consortium (PCIC, 2017). Downscaling is necessary to apply the coarse-scale GCM results (ranging from 1.1° to 3.7° in longitude and 0.9° to 2.8° in latitude; Supplementary Table 1) at the finer scale of the hydrologic model configured at 0.25° horizontal resolution in both latitude and longitude. The downscaling process also corrects GCM biases in temperature and precipitation relative to observations.

PCIC used the so-called "ANUSPLIN" station-based daily gridded climate dataset (Hutchinson et al., 2009; Hopkinson et al., 2011; NRCan, 2014; ANUSPLIN refers to the gridding technique, which is based on the Australian National University spline interpolation method) as the downscaling target (described below). This dataset contains gridded daily maximum and minimum air temperature (°C), and total daily precipitation (mm) data for the Canadian landmass having a spatial resolution of about 9.26 km in the meridional direction and one that varies proportionally to the cosine of latitude in the zonal direction. Daily wind speed grids are interpolated from coarse-scale (2.5° latitude × 2.5° longitude) daily wind speeds at a 10-m height above ground from the National Centers for Environmental Prediction/National Center for Atmospheric Research (NCEP/NCAR) Reanalysis (Kalnay et al., 1996).

Downscaling was performed with the Bias Correction/Constructed Analogue Quantile Mapping method, version 2.0 (BCCAQ2), a hybrid approach that combines the bias corrected constructed analogues (BCCA; Maurer et al., 2010) and bias corrected climate imprint (BCCI; Hunter and Meentemeyer, 2005) techniques. BCCA bias-corrects the large-scale daily GCM temperature and precipitation using quantile mapping to a target gridded observational product (here, ANUSPLIN), aggregated to the GCM grid-scale and then integrates spatial information by regressing each daily large-scale temperature or precipitation field on a collection of fine-scale historical analogues selected from

ANUSPLIN. Using this relationship, fine-scale patterns are generated from the target dataset. In parallel, BCCI applies quantile mapping to daily GCM outputs that have been interpolated to the high-resolution grid based on "climate imprints" derived from long-term ANUSPLIN climatologies (Hunter and Meentemeyer, 2005). BCCA produces results that may be subject to insufficient temporal variability whereas BCCI can contain artifacts due to spatial smoothing. In BCCAQ, daily values within a given month from BCCI are reordered according to their corresponding ranks in BCCA, improving the spatiotemporal variability (Werner and Cannon, 2016). BCCAQ2 further refines BCCAQ by the substitution of quantile delta mapping instead of regular quantile mapping in BCCI to preserve the magnitude of projected changes over all quantiles from the GCM in the downscaled output (Cannon et al., 2015). The CMIP5 projections were initially downscaled from the native GCM resolutions to the 0.0833° resolution of ANUSPLIN, then averaged to a resolution of 0.25° to match the VIC model grid.

2.3 Variable Infiltration Capacity (VIC) Model and Simulation Strategy

The semi-distributed macroscale Variable Infiltration Capacity (VIC) model (Liang et al., 1994, 1996) was used to simulate hydrological processes in the FRB. The VIC model conserves surface water and energy balances for large-scale watersheds such as the FRB (Cherkauer et al., 2003). In addition to the daily meteorological forcings mentioned in Sec. 2.2, the model also requires a number of static gridded fields to characterize soil type, vegetation type, and elevation. VIC simulates the sub-grid variability by dividing each gridcell into several elevation bands (Nijssen et al., 2001a) each of which is further subdivided into a number of tiles that represent different land surface types, producing a matrix delineated by topography and land surface type. Energy and water balances and snow are determined for each tile separately (Gao et al., 2009). The VIC model is coupled (offline) to a routing scheme adapted

Hydrol. Earth Syst. Sci. Discuss., https://doi.org/10.5194/hess-2018-232
Manuscript under review for journal Hydrol. Earth Syst. Sci.
Discussion started: 14 May 2018

from Wu et al. (2011) that approximates the known channel network runoff from gridcells (accumulated from tiles within grid boxes). Streamflow produced in this way is extracted at outlet points of specific sub-basins of interest (Lohmann et al., 1996, 1998a, b).

The VIC model has been commonly applied to assess water resources, land–atmosphere interactions and hydrological responses over various river basins globally (e.g., Nijssen et al., 2001a, b; Haddeland et al., 2007; Adam et al., 2009; Cuo et al., 2009; Elsner et al., 2010; Gao et al., 2010; Wen et al., 2011, Zhou et al., 2016). It has been extensively used for climate change research due to its process-based structure that allows the model to respond to changing air temperature and precipitation in a more physically realistic way than empirically-based or lumped models. It is also used to evaluate climate change driven hydrologic responses in the basins having snowmelt-dominant runoff (Christensen and Lettenmaier, 2007; Hidalgo et al., 2009; Cherkauer and Sinha, 2010; Schnorbus et al., 2011; Islam et al., 2017). It has been successfully implemented, calibrated and evaluated for the FRB as reported in Shrestha et al. (2012), Kang et al. (2014), Islam et al. (2017) and Islam and Déry (2017).

Calibration and validation of the VIC model for this study was conducted through retrospective hydrologic simulations from 1979 to 2006 using ANUSPLIN re-gridded to the VIC grid directly. Figure 2 describes the full experimental setup while further details of the VIC model implementation and application to the FRB are described in Islam et al. (2017) and Islam and Déry (2017). The calibrated VIC model was integrated at a daily time step from 1950 to 2099 using statistically-downscaled daily precipitation, maximum and minimum air temperature from each of the 21 downscaled CMIP5 GCM simulations (using historical and RCP 8.5 forcing) at 0.25° horizontal resolution. Three 30-year periods

Hydrol. Earth Syst. Sci. Discuss., https://doi.org/10.5194/hess-2018-232
Manuscript under review for journal Hydrol. Earth Syst. Sci.
Discussion started: 14 May 2018

were analysed in detail: the 1990s (1980 to 2009), 2050s (2040 to 2069) and 2080s (2070 to 2099). Relative changes were computed using the 1990s as a base period. Each simulation was initialized by running VIC for five years using the 1950 meteorological forcings to allow the model to spin-up.

2.4 Analysis Methods

2.4.1 Analysed Variables

The analysis focused primarily on VIC simulated daily values of total runoff computed as the sum of baseflow and surface runoff at each model gridcell as VIC does not simulate sub-surface flows between gridcells. At the basin's outlet, routed streamflow was converted to areal runoff by dividing it by the corresponding basin or sub-basin area and then converting it to precipitation equivalent units. To support our results of projected changes in runoff, several other variables such as total precipitation (snowfall and rainfall) and air temperature forcings and VIC simulated SWE and snowmelt were also evaluated. Snowfall and rainfall variables were extracted from VIC output. VIC uses specified air temperature thresholds to determine precipitation phase. In the current implementation, total precipitation was partitioned into 100% rainfall for temperature above 1.5°C, 100% snowfall for temperatures below -0.5°C and a mixture of rainfall and snowfall for temperatures between these two thresholds.

We defined the snow accumulation season as the days of the cold season when daily SWE accumulations, the difference between daily snow accumulation and snow melt, are >1 mm. Analyses were performed using the water year, defined here as 1 October to 30 September of the following calendar year, while the cold season was defined as the period from 1 October to 31 March. Peak runoff

Hydrol. Earth Syst. Sci. Discuss., https://doi.org/10.5194/hess-2018-232
Manuscript under review for journal Hydrol. Earth Syst. Sci.
Discussion started: 14 May 2018

during the cold season was computed between 1 October and 1 March when the 3-day running mean daily air temperature exceeds 0°C at each gridcell.

2.4.2 Mean and Variability Calculations

Despite bias correction via the BCCAQ2 downscaling, individual climate model simulations contain structural uncertainties related to their finite resolution, solution methods, and sub-grid scale parameterizations, which constitute irreducible errors unique to each model. Considering each model realization as a valid approximation to the real climate, the spread of the multi-model ensemble (MME) allows us to quantify the uncertainty of the modelling approach. We used the MME to quantify changes in the climatological mean and interannual variability. Standard deviation is used to estimate the interannual variability considering that it provides a straightforward computation of variation of the distribution. First, the mean climatology was calculated for each model as:

$$\bar{x}_i = \frac{1}{T}\sum_{t=1}^{T} x_{it} \quad (1)$$

where x is the variable of interest, i indicates ensemble member and t represents time. The interannual standard deviation S_i for each model was calculated as:

$$S_i = [\frac{1}{T-1}\sum_{t=1}^{T}(x_{it} - \bar{x}_i)^2]^{\frac{1}{2}} \quad (2)$$

Using Eqs. (1) and (2), the MME mean climatology $\bar{x}$ and MME mean standard deviation $\bar{S}$ was then calculated as:

Hydrol. Earth Syst. Sci. Discuss., https://doi.org/10.5194/hess-2018-232
Manuscript under review for journal Hydrol. Earth Syst. Sci.
Discussion started: 14 May 2018

$$\bar{x} = \frac{1}{I}\sum_{i=1}^{I}\bar{x}_i \tag{3}$$

$$\bar{S} = \frac{1}{I}\sum_{i=1}^{I}S_i \tag{4}$$

where I = 21 is the number of simulations. The inter-model spread in $\bar{x}$ and $\bar{S}$ was estimated by a 5-95% confidence interval. Equation (2) was used to calculate annual (or cold season) variability within each 30-year time period by evaluating the interannual standard deviation for each day of the water year in the 1990s, 2050s and 2080s time periods. Equations (3) and (4) were used for both the MME mean and the MME mean interannual standard deviation.

The effect of transient warming in the 2050s and 2080s in the RCP8.5 scenario was removed by subtracting the least squares linear trend from each time series before calculating its variability. Variability in 7-day runoff was also computed using a 7-day running window from daily runoff time series.

The 5% and 95% lower and upper bounds for 90% confidence intervals of the MME mean were calculated using the standard deviation among ensemble members where the degrees of freedom are the ensemble members (I-1). A t-test statistic ($p < 0.05$) was used to test the significance of the linear regression slopes.

2.5 Snowmelt Pulse Detection

The changes in runoff variability associated with warming and changes in precipitation phase provide evidence of changing flow regimes in the FRB. We used Snowmelt Pulse (SP) detection (Cayan et al., 2001; Fritze et al., 2011) to investigate the potential for transitions to new hydrological regimes in the basins of interest. The SP date, which is defined as the day when the cumulative departure from that water year's mean flow is most negative, provides a way for determining the time at which increased ablation in a snowmelt-dominant basin initiates the transition from low winter base flows to high spring flow (freshet) conditions. While accumulation of flow departures commenced for each water year on 1 October, we only considered those SPs occurring between 1 March (water-day 151 (152 for leap years)) and 15 June (water-day 238 (239 for leap years)) so as to exclude runoff pulses induced by rainfall events outside the (present-day) freshet period. We also ignored SPs when the ratio of the area of positive cumulative flow departure (indicating rainfall events) to the area of negative departure between water-days 151 and 238 was greater or equal to unity, as this also indicates rainfall-dominant runoff.

As an illustration, we applied the algorithm to different river flow regimes using daily observed data acquired from the Water Survey of Canada's Hydrometric Dataset (HYDAT; Water Survey of Canada, 2018). As an example, we show the cumulative departures from annual mean flow for two distinct flow regimes, i.e. Capilano River Above Intake (Fig. 3a) and Fraser River at Hope (Fig. 3b) for selected years in the 1914-2010 period. The application of the algorithm reveals the presence of a SP in the Fraser River at Hope in all selected years, while for the Capilano River, an example of a rainfall-dominant system, SPs are quite rare.

Hydrol. Earth Syst. Sci. Discuss., https://doi.org/10.5194/hess-2018-232
Manuscript under review for journal Hydrol. Earth Syst. Sci.
Discussion started: 14 May 2018

Hydrology and Earth System Sciences
Open Access
Discussions

To explore potential regime changes in the FRB, we evaluated and compared the fraction of years for which SPs were recorded within each analysis period (1990s, 2050s, 2080s), for each 0.25° gridcell and for all CMIP5-VIC simulations (with sample size of 21 CMIP-VIC simulations × 30 years = 630 years). In each simulation, each gridcell was classified into one of four snow-dominant categories (SDCs) as defined by Fritze et al. (2011): SDC1 (clearly rain-dominant: SP occurrence in < 30% of water years); SDC2 (mostly rain-dominant, SP occurrence ≥ 30% but < 50%); SDC3 (mostly snowmelt-dominant, SP occurrence ≥ 50% but < 70%); and SDC4 (clearly snowmelt-dominant, SP occurrence ≥ 70%). This allowed comparisons of projections for the 2050s and 2080s and spatial distributions of gridcells in each SDC relative to those from the 1990s base period. Finally, the SDC results were aggregated by geoclimatic region.

3 Results

We examine first the projected changes in the mean and interannual variability of precipitation over the FRB. Next we explore the consequences of these changes for runoff means and variability at various temporal and spatial scales. This is followed by a discussion of changing flow regimes over the FRB at regional and sub-basin scales.

3.1 Projected Changes in Precipitation and Snow

The MME mean precipitation, spatially-averaged over the FRB's gridcells, increases by nearly 15% in the 2080s relative to the 1990s base period both in annual mean and in the cold season (Fig. 4a, b). The changes are largest in the northern FRB (Supplementary Fig. 1a, c) reaching up to 20% in the cold season (Supplementary Fig. 1c). The MME mean precipitation variability increases continuously with

Hydrology and Earth System Sciences
Open Access
Discussions

warming when spatially-averaged over the whole FRB (Fig. 4a, b). The relationship between precipitation variability and FRB mean temperature is almost linear with a rate of change of about 4% $°C^{-1}$ towards the end of the 21st century compared to the 1990s. The rate of change of precipitation interannual variability is as large as the MME mean precipitation. Precipitation variability increases more substantially in the cold season (Fig. 4b) with increases of ~20% to ~80% in the interior and northern FRB (Supplementary Fig. 1d). In the cold season, the increase in interannual variability is greater than that in mean precipitation. Such increases in the precipitation variability under the projected air temperature increase suggest a somewhat more variable future climate at the end of this century.

The partitioning of MME mean total precipitation into rainfall and snowfall reveals substantial increases in daily rainfall towards the end of the 21st century across the Coast Mountains, Interior Plateau and Rocky Mountains (Fig. 5a, c, e). The increase in rainfall emerges prominently in the Coast Mountains in the latter half of the 21st century, especially in the cold season. Simultaneously, snowfall decreases (Fig. 5b) markedly in this region, which can be attributed to reduced frequency of future subfreezing air temperatures. Decreases in snowfall also occur in the Interior Plateau and Rocky Mountains (Fig. 5d, f) where the latter remain more resilient to snowfall declines probably due to cold conditions at higher elevations.

Warm temperatures and reduced snowfall induce considerable changes in the snow accumulation and ablation seasons and in snowmelt (Fig. 6). SWE accumulation and its seasonality decline towards the end of the 21st century, with more prominent changes in the Coast Mountains relative to other regions (Fig. 6a). The length of the snow accumulation season shortens by about 38%

on average in the 2080s for all geoclimatic regions relative to the 1990s base period with a reduction from nearly 80 to 50 days in the Coast (Fig. 6a) and Rocky Mountains (Fig. 6e), and from 65 to 40 days in the Interior Plateau (Fig. 6c). The magnitude and seasonality of snowmelt (Fig. 6b, d, f), which is responsible for generating high flows typically in May or June, shows earlier snowmelt freshets in the future and decreases in snowmelt volume. Changes in the partitioning of precipitation between rainfall and snowfall greatly impact the seasonal SWE distribution consistent with the findings of Islam et al. (2017). While snowmelt events diminish in the future overall, snowmelt events begin to appear during the cold season in the Coast Mountains (Fig. 6b) towards the end of the 21st century, possibly due to increases in rain-on-snow events.

3.2 Projected Changes in Runoff Variability and Seasonality

As with precipitation variability, the FRB's runoff variability changes systematically with warming both in the annual mean and in the cold season (Fig. 4c, d). The change in the cold season runoff variability is driven by both the warming and increase in precipitation and its variability.

The MME projected hydrograph for the Fraser River at Hope shows more runoff in the late winter and spring owing to the earlier onset of spring snowmelt, which advances by nearly 25 days (consistent with Islam et al., (2017)) in the 2050s and 40 days in the 2080s relative to the 1990s (Fig. 7a). The magnitudes of the annual peak and post-peak flows are, however, progressively diminished in the future periods, with reduced discharge until early October. These changes imply earlier recession to progressively lower flows in summer when salmon are migrating up the Fraser River. Daily mean runoff in the UF, QU, TN and CH sub-basins exhibits similar features of future change (Supplementary

Fig. 2). The advance in the timing of the annual peak flow in these sub-basins is slightly less than for the FRB as a whole (~20 days for UF, ~18 days for QU, ~25 days for TN and ~35 days for CH), presumably due to their higher mean elevations. CH features a later freshet (by ~35 days) in the base period compared to the other three sub-basins. This reflects the fact that its flow is partially controlled by the Coast Mountains with influence from the Pacific Ocean along with the presence of large lakes and extensive glaciers in the basin. While the CH sub-basin also features an advance of peak runoff in the future, it exhibits only slightly reduced peak flow magnitudes, unlike the other sub-basins and the FRB as a whole (Supplementary Fig. 2j and Fig. 7a).

In the Rocky Mountains and Interior Plateau along with the UF, QU, TN and LF sub-basins, annual runoff remains stable or increases slightly (Supplementary Table 2) but cold season runoff increases substantially (Table 1). In the Coast Mountains and the CH sub-basin, cold season runoff increases in the future owing to robust rainfall increases year-round. The drainage area mean cold season runoff for the Fraser River at Hope increases from 83±2 mm yr^{-1} in the 1990s to 142±10 mm yr^{-1} in the 2080s (Table 1). The substantial increase in cold season runoff accompanies corresponding increases in interannual variability by the end of this century (Table 1).

The changes in daily runoff variability (interannual variability of each day of water year) are modest in summer with small decreases that are consistent with corresponding runoff decreases (Fig. 7b). In contrast, variability increases substantially in the cold season with greater increases in the 2080s than in the 2050s for the Fraser River at Hope (Fig. 7b). Similar changes also emerge in the UF, QU, TN and CH sub-basins exhibiting increasing cold season variability with magnitudes comparable to the

LF (Supplementary Fig. 2). The changes in daily variability in 7-day moving windows of daily runoff are fairly large in the cold season (Fig. 7c) revealing increased day-to-day flow fluctuations along with an increase in the interannual variability of daily variability in the 2050s and 2080s.

The geographic distribution of the change in runoff mean and interannual variability reveals increases in cold season mean runoff across most of the gridcells in the FRB, with more than 100% increase in many gridcells in the 2080s (Fig. 8c). The runoff variability consistently increases from the 2050s to the 2080s relative to the 1990s with maximum increases of ~80% to 120% in the 2050s and ~100% to 200% in the 2080s over the whole FRB (Fig. 8b, d). The slope is significantly positive between changes in cold season variability and elevations in each gridcell in the Coast Mountains and Interior Plateau geoclimatic regions revealing increasing runoff variability with rising elevations (Supplementary Fig. 3). The Rocky Mountains exhibit strong negative elevation dependency of runoff variability with a 30% reduction in runoff variability with every 1 km increase in elevation during the 2080s.

The future evolution of the annual cycle of daily runoff shows that while the dominant snowmelt-generated peak flow shifts earlier by ~1 month, noticeable cold season runoff events emerge in winter and spring at the end of the 21st century (Fig. 9). This is most pronounced in the Coast Mountains where fall-winter runoff events rival the summer peak runoff in magnitude (Fig. 9a). The spatially-averaged runoff over the Coast Mountains further highlights the strong increase in cold season peak runoff in this region (Supplementary Fig. 4). Apart from the increase in cold season peak runoff magnitude and its annual variability, the corresponding peak flow occurs later with warming in the

Coast Mountains, from late November (~water-day 50) to the beginning of December (~water-day 60) at the end of 21st century (Supplementary Fig. 4b). Overall, as the climate warms, the cold season peak runoff date occurs later in the water year, and thus peak runoff also occurs later. Such increase in cold season peak runoff magnitudes are simulated by most CMIP5-VIC simulations (Supplementary Fig. 4c).

3.3 Changes in Runoff Regimes

Potential future changes in FRB flow regimes are assessed using the SP detection algorithm described in Sec. 2.5. SPs occur in the VIC simulations in all years at nearly most of the gridcells in the 1990s base period (Fig. 10), resulting in an SDC4 flow regime classification throughout the basin except in the lower Fraser valley. The number of SPs decreases in future periods with the maximum change occurring in the Interior Plateau (Fig. 10), where frequency declines from 100% to only 43% snow-dominant in the 2080s (Table 2). The Rocky and Coast Mountains decline to 64% and 57% snowmelt-dominant systems by the 2080s. The corresponding uncertainties in these declines are 7%, 6% and 4% for Interior Plateau, Rocky and Coast Mountains, respectively. In contrast with the spatially-averaged response of the geoclimatic regions, routed flow at the UF, QU, TN, CH and LF shows a weaker transition of flow regimes (Table 2 and Supplementary Fig. 5).

The spatial classification of SP changes (Fig. 11) shows most of the Interior Plateau transitioning from snowmelt-dominant SDC4 to rainfall-dominant SDC1 (33% gridcells) or SDC2 (26% gridcells) by the end of this century. By contrast, mountainous regions such as the Rocky Mountains show resilience to regime transitions compared to lower elevations and remain mostly snowmelt-dominant SDC3 (14% gridcells) or SDC4 (58% gridcells) in the 2080s. In the Coast Mountains, the higher elevations resist regime transitioning compared to the remainder of the areas having robust transitions to rainfall-dominant SDC1 or SDC2.

4 Discussion and Conclusion

The overall question driving this study is how future projected increases in air temperature and precipitation mean along with changes in precipitation phase and variability will modulate the FRB's runoff variability and flow regimes. To this end, we used VIC simulations, driven by statistically downscaled CMIP5 model projections, to analyse the magnitude, timing and variability of simulated runoff in different sub-basins and geoclimatic regions within the FRB. Furthermore, we used a SP detection algorithm to identify the transition of snowmelt-dominant to rainfall-dominant regimes.

4.1 Projected changes in runoff mean

Analysis of contemporary and future climate and hydrological simulations suggests that warming and changes in precipitation variability (Fig. 4) and phase (Fig. 5) will lead to a significant decline in cold season snowpack accumulation and shift spring snowmelt earlier (Fig. 6). The projected change in the runoff mean is sensitive to changes in both the mean and variability of precipitation in a warming climate. These findings are consistent with a recent study by Pendergrass et al. (2017) reporting a global increase of precipitation variability in CMIP5 models simulations on both interannual and daily timescales. Projected increases in the precipitation rain-to-snow fraction will have a strong impact on the severity of flooding, for example on mountainsides, with increased spring rainfall accelerating snowmelt runoff.

Despite advances in annual maximum runoff (Fig. 7a), the total annual runoff in most sub-basins does not change substantially (Supplementary Table 2). The stability of total annual runoff implies that a projected increase in rainfall fraction and seasonality will induce considerable changes in runoff timing. The absolute magnitudes of both SWE change and snowmelt are higher in the Coast Mountains (Fig. 6) compared to the Rocky Mountains, likely because the latter region will continue to have cold continental winters with future mean temperatures well below 0°C. Changes in SWE magnitude and seasonality in all three geoclimatic regions shift runoff timing earlier in spring and summer (Fig. 7). Increased cold season precipitation implies more water input to the basin and thus more intense peak flows. In contrast, warmer temperatures reduce the cold season snow and shorten the snow accumulation season hence moderating the snowmelt-driven peak flows in summer.

Annual peak flows in the FRB's Coast Mountains will shift earlier by around one month and more frequent cold season runoff events will rival spring freshet flows in magnitude by the end of the 21st century (Fig. 7). The variability of cold season peak flows, linked to rainfall events, will also increase in the Coast Mountains. Furthermore, future increase of rainfall events accelerating snowmelt, may also contribute to increasing runoff variability in cold seasons. Enhanced atmospheric rivers simulated in the CMIP5 models (Warner et al., 2015) may also increase rainfall events in the Coast Mountains. Along the North American west coast, the CMIP5 models simulate higher numbers of heavy rainfall events associated with atmospheric rivers in future time periods when compared to the historical frequency. These strong increases in atmospheric moisture transport result in higher rainfall amounts in the CMIP5 ensemble which, in turn, produce increased cold season runoff in the VIC simulations of the FRB. These future increases in cold season runoff may increase the risk of extreme flooding in the Coast Mountains and in the lower Fraser Basin (Curry et al., 2018, in preparation). The current water management strategies (flood planning, water storage, etc.), particularly on the southwest coast of BC, will need to be bolstered to cope with projected increases in cold season peak flow events and variability.

Future changes in the FRB's runoff peak flows will also impact salmon life cycles at the stream level. Studies have observed an inverse relationship between salmon spawning survival and higher flows due to the scouring mortality of spawns caused by high runoff in increased rainfall periods (Thorne and Ames 1987; Steen and Quinn 1999; Martins et al., 2012). The projected increase in rainfall and consequently higher flows could increase the scouring mortality of sockeye salmon causing population reductions. Furthermore, the considerable changes in future flows may substantially increase physiological stress during up-river salmon migrations into the FRB and thus further degrade their reproduction rates.

4.2 Projected changes in runoff variability

The analysis of the annual cycle of 7-day variability in daily runoff shows evidence of greater day-to-day fluctuations in Fraser River flows in the 2050s and 2080s relative to the 1990s base period (Fig. 7c). The peak day-to-day variability, occurring mainly in October, intensifies in the future along with a shift towards November. Such increases in the magnitude, variability and shifts in its timing come from projected changes in precipitation phases (Fig. 5) and increases in cold season snowmelt events (Fig. 6). The projected changes in day-to-day flow variability in the summer probably arise from changes in the magnitude and timing of the spring freshet. Accelerated and earlier snowmelt may result in flashier flows causing the increase for potential flooding or attenuated spring freshet with attendant drought potential in summer. Furthermore, grid-scale projected changes in runoff variability are strongly dependent on the elevation (Supplementary Fig. 3). Higher elevations in the Coast Mountains will experience greater changes in runoff variability compared to lower elevations of the Interior Plateau. The main factors controlling cold season runoff variability are the changes in precipitation means and variability. This suggests that precipitation variability will contribute to more intense cold season runoff variability (Fig. 4) in addition to any increase that may be due to higher temperatures.

4.3 Transitions between runoff regimes

Based on the results of the SP detection analysis, the FRB will transition to a less snowmelt-dominated regime in the 21st century. The Interior Plateau will transition from snow-dominant to increasingly rain-dominant regimes (Table 2 and Fig. 10). Changes in the snow-dominant category arise more prominently across the Interior Plateau owing to its lower mean elevation with smaller snowpack accumulation in winter and thus higher sensitivity to changes in air temperature during the cold season. Snowpack declines are most pronounced at temperatures near freezing that occur more often at Interior Plateau lower elevations during fall or spring.

In FRB mountainous regions, flow regimes depend mainly on the proximity to marine influences and elevation, with higher elevations having cooler air temperatures and thus longer periods of snow accumulation. Therefore the snowpack declines are less sensitive to temperature change in the Rocky Mountains with a possibility of experiencing increased snowfall due to higher moisture availability.

Future percentages of SP years for all sub-basins are considerably larger than the spatially-averaged values of the geoclimatic regions overlapping them (Table 2). The former, computed at basin outlets, are sensitive to the channel network and the routing model used to route these sub-basin flows. In the routing procedure, the model gridcells contributing flows to the outlet gauge occupy mostly higher elevations and hence produce flow statistics with more SPs. This attenuation of the climate change signal at channel outlets is consistent with the recent finding of Chezik et al. (2017) reporting river networks dampen local hydrologic signals of climate change since the regional characteristics of the channel network aggregate the upstream climate at different spatial scales.

Overall, future projected changes in precipitation, SWE and runoff are in good qualitative agreement with the results of Islam et al. (2017), who used a smaller MME and a different downscaling procedure. In this work, we take advantage of a larger MME with more realistic daily timescale variability to investigate future changes in runoff variability and seasonality. It should be noted, however, that all of the historical CMIP5 driving data are essentially constrained to have the observed means and variability for the historical period in the statistical downscaling. The historical period variability therefore does not reflect large inter-model differences. Future variability does see the influence of inter-model differences and not just changes in variability due to forced climate change. The increase in the runoff variability may be therefore somewhat overestimated in our analysis. However, considering the lower inter-model spread compared to the MME mean in the cold season (Table 1), these changes are mainly induced by projected climate change with increased precipitation variability. Such an increase in precipitation variability is also reported in other studies (see Pendergrass et al., 2017) using CMIP5 MME precipitation without any downscaling method.

Besides the downscaling methodology, the GCM dynamics, natural climate variability and hydrological modelling all form sources of uncertainty in this study's projected hydrological changes. Furthermore, the hydrological model used in this study is integrated on a relatively coarse resolution (0.25°), which may not represent small-scale dynamics related to the FRB's complex topography.

Acknowledgments

This work was supported by the Natural Sciences and Engineering Research Council of Canada (NSERC) funded Canadian Sea Ice and Snow Evolution (CanSISE) Network, the Mountain Water Futures (MWF) initiative of the Global Water Futures (GWF) program and the Nechako Environmental Enhancement Fund (NEEF). Thanks to colleagues from the Pacific Climate Impacts Consortium for their assistance and contributions in the VIC model implementation. The authors thank Michael Allchin (UNBC) for plotting Fig. 1a and for providing useful comments. The authors acknowledge the World Climate Research Programme's Working Group on Coupled Modelling, which is responsible for CMIP5, and thank the climate modelling groups for producing and making available their GCM output. For CMIP, the U.S. Department of Energy's Program for Climate Model Diagnosis and Intercomparison provides coordinating support and led development of software infrastructure in partnership with the Global Organization for Earth System Science Portals.

References

Adam, J. C., Hamlet, A. F. and Lettenmaier, D. P.: Implications of global climate change for snowmelt hydrology in the twenty-first century, Hydrol. Process., 23, 962–972, doi:10.1002/hyp.7201, 2009.

Benke, A. C. and Cushing, C. E.: Rivers of North America, Elsevier Press, New York, 607-732, 2005.

Cannon, A. J., Sobie, S. R. and Murdock, T. Q.: Bias correction of GCM precipitation by quantile mapping: How well do methods preserve changes in quantiles and extremes? J. Climate, 28, 6938-6959, 2015.

Cayan, D., Kammerdiener, S., Dettinger, M., Caprio, J. and Peterson, D.: Changes in the onset of spring in the western United States. Bull. Amer. Meteor. Soc., 82, 399–415, 2001.

Cherkauer, K. A. and Sinha, T.: Hydrologic impacts of projected future climate change in the Lake Michigan region, J. Great Lakes Res., 36(SUPPL. 2), 33–50, doi:10.1016/j.jglr.2009.11.012, 2010.

Cherkauer, K. A., Bowling, L. C. and Lettenmaier, D. P.: Variable infiltration capacity cold land process model updates, Glob. Planet. Change, 38(1–2), 151–159, doi:10.1016/S0921-8181(03)00025-0, 2003.

Chezik, K. A., Anderson, S. C. and Moore, J. W.: River networks dampen long-term hydrological signals of climate change, Geophys. Res. Lett., 44(14), 7256–7264, doi:10.1002/2017GL074376, 2017.

Christensen, N. S. and Lettenmaier, D. P.: A multimodal ensemble approach to assessment of climate change impacts on the hydrology and water resources of the Colorado River Basin, Hydrol. Earth Syst. Sci., 11, 1417–1434, 2007.

Collins, M., Knutti, R., Arblaster, J., Dufresne, J.-L., Fichefet, T., Friedlingstein, P., Gao, X., Gutowski, W. J., Johns, T., Krinner, G., Shongwe, M., Tebaldi, C., Weaver, A. J. and Wehner, M.: Long-term Climate Change: Projections, Commitments and Irreversibility, in Climate Change 2013: The Physical Science Basis. Contribution of Working Group I to the Fifth Assessment Report of the Intergovernmental Panel on Climate Change, pp. 1029–1136, 2013.

Cuo, L., Lettenmaier, D. P., Alberti, M. and Richey, J. E.: Effects of a century of land cover and climate change on the hydrology of the Puget Sound basin, Hydrol. Process., 23(6), 907–933, doi:10.1002/hyp.7228, 2009.

Curry, C., Islam, S., Zwiers F., Déry, S. J.: The changing character of extreme streamflow in the Fraser Basin in the 21st century, in preparation, 2018.

Danard M. and Murty, T. S.: On recent climate trends in selected salmon-hatching areas of British Columbia. J. Climate, 7, 1803–1808, doi:10.1175/1520-0442(1994)007,1803: ORCTIS.2.0.CO;2, 1994.

Déry, S. J., Hernández-Henríquez, M., Owens P. N., Parkes M. W. and Petticrew E. L.: A century of hydrological variability and trends in the Fraser River Basin, Environ. Res. Lett., 7(2), 024019, doi:10.1088/1748-9326/7/2/024019, 2012.

Eliason, E. J., Clark, T. D., Hague, M. J., Hanson, L. M., Gallagher, Z. S., Jeffries, K. M., Gale, M. K., Patterson, D. A., Hinch, S. G. and Farrell, A. P.: Differences in thermal tolerance among sockeye salmon populations, Science, 332(6025), 109–112, doi:10.1126/science.1199158, 2011.

Elsner, M. M., Cuo, L., Voisin, N., Deems, J. S., Hamlet, A. F., Vano, J. A., Mickelson, K. E. B., Lee, S. Y. and Lettenmaier, D. P.: Implications of 21st century climate change for the hydrology of Washington State, Clim. Change, 102(1–2), 225–260, doi:10.1007/s10584-010-9855-0, 2010.

Ferrari, M. R., Miller, J. R. and Russell, G. L.: Modeling changes in summer temperature of the Fraser River during the next century, J. Hydrol., 342(3-4), 336–346, doi:10.1016/j.jhydrol.2007.06.002, 2007.

Fritze, H., Stewart, I. T., and Pebesma, E.: Shifts in western North American snowmelt runoff regimes for the recent warm decades, J. Hydrometeorol., 12, 989–1006, 2011.

Gao, H., Tang, Q., Ferguson, C. R., Wood, E. F. and Lettenmaier, D. P.: Estimating the water budget of major US river basins via remote sensing, Int. J. Remote Sens., 31(14), 3955–3978, doi:10.1080/01431161.2010.483488, 2010.

Gao, H., Tang, Q., Shi, X., Zhu, C., Bohn, T. J., Su, F., Sheffield, J., Pan, M., Lettenmaier, D. P. and Wood, E. F.: Water Budget Record from Variable Infiltration Capacity (VIC) Model. In Algorithm Theoretical Basis Document for Terrestrial Water Cycle Data Records (unpublished), 2009.

Haddeland, I., Skaugen, T. and Lettenmaier, D. P.: Hydrologic effects of land and water management in North America and Asia: 1700-1992, Hydrol. Earth Syst. Sci., 11(2), 1035–1045, doi:10.5194/hess-11-1035-2007, 2007.

Hidalgo, H. G., Das, T., Dettinger, M. D., Cayan, D. R., Pierce, D. W., Barnett, T. P., Bala, G., Mirin, A., Wood, A. W., Bonfils, C., Santer, B. D. and Nozawa, T.: Detection and attribution of streamflow timing changes to climate change in the western United States, J. Climate, 22(13), 3838–3855, doi:10.1175/2009JCLI2470.1, 2009.

Hildebrand, L. R., Drauch Schreier, A., Lepla, K., McAdam, S. O., McLellan, J., Parsley, M. J., Paragamian, V. L. and Young, S. P.: Status of White Sturgeon (Acipenser transmontanus

Richardson, 1863) throughout the species range, threats to survival, and prognosis for the future, J. Appl. Ichthyol., 32, 261–312, doi:10.1111/jai.13243, 2016.

Hopkinson, R. F., McKenney, D. W., Milewska, E. J., Hutchinson, M. F., Papadopol, P. and Vincent, L. A.: Impact of aligning climatological day on gridding daily maximum-minimum temperature and precipitation over Canada, J. Appl. Meteorol. Climatol., 50(8), 1654–1665, doi:10.1175/2011JAMC2684.1, 2011.

Hunter, R. D., and Meentemeyer, R. K.: Climatologically aided mapping of daily precipitation and temperature. J. Appl. Meteorol., 44, 1501-1510, 2005.

Hutchinson, M. F., McKenney, D. W., Lawrence, K., Pedlar, J. H., Hopkinson, R. F., Milewska, E. and Papadopol, P.: Development and testing of Canada-wide interpolated spatial models of daily minimum–maximum temperature and precipitation for 1961–2003, J. Appl. Meteorol. Climatol., 48(4), 725–741, doi:10.1175/2008JAMC1979.1, 2009.

Islam, S. U., and Déry, S. J.: Evaluating uncertainties in modelling the snow hydrology of the Fraser River Basin, British Columbia, Canada, Hydrol. Earth Syst. Sci., 21(3), 1827–1847, doi:10.5194/hess-21-1827-2017, 2017.

Islam, S. U., Déry, S. J., and Werner, A. T.: Future climate change impacts on snow and water resources of the Fraser River Basin, British Columbia, J. Hydrometeorol., 18(2), 473-496, doi:10.1175/JHM-D-16-0012.1, 2017.

Kalnay, E., Kanamitsu, M., Kistler, R., Collins, W., Deaven, D., Gandin, L., Iredell, M., Saha, S., White, G., Woollen, J. and Zhu, Y.: The NCEP/NCAR 40-year reanalysis project, Bull. Amer. Meteorol. Soc., *77*, 437-471, 1996.

Kang, D. H., Gao, H., Shi, X., Islam, S. U. and Déry, S. J.: Impacts of a rapidly declining mountain snowpack on streamflow timing in Canada's Fraser River Basin, Sci. Rep., 6, 19299, doi:10.1038/srep19299, 2016.

Kang, D. H., Shi, X., Gao, H. and Déry, S. J.: On the changing contribution of snow to the hydrology of the Fraser River Basin, Canada, J. Hydrometeorol., 15(4), 1344–1365, doi:10.1175/JHM-D-13-0120.1, 2014.

Labelle, M.: Status of Pacific Salmon Resources in Southern British Columbia and the Fraser River Basin. Vancouver, BC: Pacific Fisheries Resource Conservation Council. (http://www.dfo-mpo.gc.ca/Library/347488.pdf, 2009.

Liang, X., Lettenmaier, D. P., Wood, E. F. and Burges, S. J.: A simple hydrologically based model of land surface water and energy fluxes for general circulation models, J. Geophys. Res. Atmos., 99(D7), 14415–14428, doi:10.1029/94JD00483, 1994.

Liang, X., Wood, E. F. and Lettenmaier, D. P.: Surface soil moisture parameterization of the VIC-2L Model: Evaluation and modifications, Glob. Planet. Chang., 13, 195–206, 1996.

Lohmann, D., Nolte-Holube, R. and Raschke, E.: A large-scale horizontal routing model to be coupled to land surface parametrization schemes, Tellus, Ser. A Dyn. Meteorol. Oceanogr., 48(5), 708–721, doi:10.1034/j.1600-0870.1996.t01-3-00009.x, 1996.

Lohmann, D., Raschke, E., Nijssen, B. and Lettenmaier, D. P.: Regional scale hydrology: I. Formulation of the VIC-2L model coupled to a routing model, Hydrol. Sci. J., 43(1), 131–141, doi:10.1080/02626669809492107, 1998a.

Lohmann, D., Raschke, E., Nijssen, B. and Lettenmaier, D. P.: Regional scale hydrology: II. Application of the VIC-2L model to the Weser River, Germany, Hydrol. Sci. J., 43(1), 143–158, doi:10.1080/02626669809492108, 1998b.

Martins, E. G., Hinch, S. G., Cooke, S. J. and Patterson, D. A.: Climate effects on growth, phenology and survival of sockeye salmon (Oncorhynchus nerka): a synthesis of the current state of knowledge and future research directions. Reviews in Fish Biology and Fisheries, 22, 887-914, 2012.

Maurer, E. P., Hidalgo, H. G., Das, T., Dettinger, M. D., and Cayan, D. R.: The utility of daily large-scale climate data in the assessment of climate change impacts on daily streamflow in California, Hydrol. Earth Syst. Sci., 14, 1125-1138, doi:10.5194/hess-14-1125-2010, 2010.

McAdam, S. O., Walters, C. J., and Nistor, C.: Linkages between white sturgeon recruitment and altered bed substrates in the Nechako River, Canada, Trans. Amer. Fish. Soc., 134, 1448-1456, 2005.

Moore, R. D.: Hydrology and water supply in the Fraser River Basin. In water in sustainable development: exploring our common future in the Fraser River Basin, AHJ Dorcey, JR Griggs (eds). Wastewater Research Centre, The University of British Columbia: Vancouver, British Columbia, Canada; 21–40, 1991.

Morrison, J., Quick, M. C. and Foreman, M. G. G.: Climate change in the Fraser River watershed: flow and temperature projections, J. Hydrol., 263(1–4), 230–244, doi:10.1016/S0022-1694(02)00065-3, 2002.

Nijssen, B., O'Donnell, G. M., Lettenmaier, D. P., Lohmann, D. and Wood, E. F.: Predicting the discharge of global rivers, J. Climate, 14(15), 3307–3323, doi:10.1175/1520-0442(2001)014<3307:PTDOGR>2.0.CO;2, 2001b.

Nijssen, B., Schnur, R. and Lettenmaier, D. P.: Global retrospective estimation of soil moisture using the Variable Infiltration Capacity land surface model, 1980–93, J. Climate, 14(8), 1790–1808, doi:10.1175/1520-0442(2001)014<1790:GREOSM>2.0.CO;2, 2001a.

NRCan.: Regional, national and international climate modelling. Retrieved from http://cfs.nrcan.gc.ca/projects/3?lang=en_CA, 2014.

Pendergrass, A. G., Knutti, R., Lehner, F., Deser, C. and Sanderson, B. M.: Precipitation variability increases in a warmer climate, Sci. Rep., 7(1), 17966, doi:10.1038/s41598-017-17966-y, 2017.

Schnorbus, M., Bennett, K. and Werner, A.: Quantifying the water resource impacts of mountain pine beetle and associated salvage harvest operations across a range of watershed scales: Hydrologic modelling of the Fraser River Basin,. Information Report: BC-X-423, Natural Resources Canada, Canadian Forestry Service, Pacific Forestry Centre, Victoria, BC, 79 pp, 2010.

Schnorbus, M., Bennett, K., Werner, A. and Berland, A. J.: Hydrologic impacts of climate change in the Peace, Campbell and Columbia sub-basins, British Columbia, Canada. Pacific Climate Impacts Consortium, University of Victoria: Victoria, BC, 157 pp., 2011.

Scott, W. B., and Crossman, E. J.: Freshwater Fishes of Canada. Bulletin 184. Fish. Res. Board Can. Bull. 184, 1–966, doi:10.1002/iroh.19760610109, 1973.

Shrestha, R. R., Schnorbus, M. A., Werner, A. T. and Berland, A. J.: Modelling spatial and temporal variability of hydrologic impacts of climate change in the Fraser River basin, British Columbia, Canada, Hydrol. Process., 26(12), 1841–1861, doi:10.1002/hyp.9283, 2012.

Steen, R. P., and Quinn, T. P.: Egg burial depth by sockeye salmon (Oncorhynchus nerka): implications for survival of embryos and natural selection on female body size. Can. J. Zool., 77(5):836–841, 1999.

Taylor, K. E., Stouffer, R. J. and Meehl, G. A.: An overview of CMIP5 and the experiment design. Bull. Amer. Meteor. Soc., 93, 485–498. doi: 10.1175/BAMS-D-11-00094.1, 2012.

Thorne, R. E., and Ames, J. J.: A note on variability of marine survival of sockeye salmon (Oncorhynchus nerka) and effects of flooding on spawning success. Can. J. Fish. Aquat. Sci., 44(10):1791–1795, 1987.

Trenberth, K. E., Dai, A., Rasmussen, R. M., and Parsons D. B.: The changing character of precipitation. Bull. Amer. Meteor. Soc., 84, 1205–1217, 2003.

Wade, N. L., Martin, J. and Whitfield, P. H.: Hydrologic and climatic zonation of Georgia Basin, British Columbia, Can. Water Resour. J., 26(1), 43–70, doi:10.4296/cwrj2601043, 2001.

Warner, M. D., Mass, C. F. and Salathé, E. P.: Changes in winter atmospheric rivers along the North American west coast in CMIP5 climate models, J. Hydrometeorol., 16(1), 118–128, doi:10.1175/JHM-D-14-0080.1, 2015.

Water Survey of Canada: HYDAT database. [Available online at http://www.ec.gc.ca/rhc-wsc/.], 2018.

Wen, L., Lin, C. A., Wu, Z., Lu, G., Pomeroy, J. and Zhu, Y.: Reconstructing sixty year (1950-2009) daily soil moisture over the Canadian Prairies using the Variable Infiltration Capacity model, Can. Water Resour. J., 36(1), 83–102, doi:10.4296/cwrj3601083, 2011.

Werner, A. T. and Cannon, A. J.: Hydrologic extremes – an intercomparison of multiple gridded statistical downscaling methods. Hydrol. Earth Syst. Sci., 20, 1483–1508, 2016.

Wu, H., Kimball, J. S., Mantua, N. and Stanford, J.: Automated upscaling of river networks for macroscale hydrological modelling, Water Resour. Res., 47(3), W03517, doi:10.1029/2009WR008871, 2011.

Zhou, T., Nijssen, B., Gao, H. and Lettenmaier, D. P.: The contribution of reservoirs to global land surface water storage variations, J. Hydrometeorol., 17, 309–325, doi:10.1175/JHM-D-15-0002.1, 2016.

Hydrology and Earth System Sciences Discussions
Open Access

Table 1: Characteristics of Water Survey of Canada (WSC) hydrometric stations and three geoclimatic regions within the FRB (Déry et al., 2012). The 30-year runoff mean and interannual variability (estimated by standard deviation) is calculated for each individual CMIP5-VIC simulation and all values are averaged to get the MME mean in the cold season. The inter-model spread in runoff mean and its interannual variability is indicated as uncertainty ranges (±) estimated by a 5-95% confidence interval.

Basin (Abbreviation) [WSC ID]	Gauged area [km^2]	Latitude [°N], Longitude [°W]	Mean elevation [m]	Mean and interannual variability of Runoff [mm yr^{-1}]					
				1990s (1980-2009)		2050s (2040-2069)		2080s (2070-2099)	
				Mean	Variability	Mean	Variability	Mean	Variability
Rocky Mountains	-	-	1567	160 ± 3	25 ± 2	205 ± 12	51 ± 7	270 ± 22	65 ± 9
Interior Plateau	-	-	1101	58 ± 0	10 ± 1	78 ± 4	19 ± 2	102 ± 7	22 ± 2
Coast Mountains	-	-	1296	450 ± 10	90 ± 7	606 ± 23	139 ± 11	730 ± 34	158 ± 15
Upper Fraser (UF) [08KB001]	32400	54.01, 122.62	1308	76 ± 8	29 ± 4	107 ± 13	46 ± 7	133 ± 18	54 ± 9
Quesnel (QU) [08KH006]	11500	52.84, 122.22	1173	119 ± 3	24 ± 2	142 ± 8	42 ± 6	182 ± 16	52 ± 7
Thompson-Nicola (TN) [08LF051]	54900	50.35, 121.39	1747	47 ± 2	13 ± 1	74 ± 7	28 ± 5	113 ± 12	38 ± 4
Chilko (CH) [08MA001]	6940	52.07, 123.54	1756	95 ± 2	20 ± 2	119 ± 6	34 ± 5	151 ± 10	42 ± 4
Fraser at Hope (LF) [08MF005]	217000	49.38, 121.45	1330	83 ± 2	13 ±1	109 ± 6	26 ± 4	142 ± 10	33 ±4

Hydrol. Earth Syst. Sci. Discuss., https://doi.org/10.5194/hess-2018-232
Manuscript under review for journal Hydrol. Earth Syst. Sci.
Discussion started: 14 May 2018

Hydrology and Earth System Sciences
Open Access
Discussions

Table 2: CMIP5-VIC simulated projected change in snowmelt-dominant regimes. Values are in % calculated using the ratio of sum of SPs years and total number of years over all 21 CMIP5-VIC simulations. The uncertainty ranges (±) indicate inter-model spread in the MME mean values indicated by a 5-95% confidence interval.

Region	**Snowmelt-Dominant Regime (%)**		
	1990s (1980-2009)	**2050s (2040-2069)**	**2080s (2070-2099)**
Rocky Mountains	100±0	88±3	64±6
Interior Plateau	100±0	73±5	43±7
Coast Mountains	95±1	74±3	57±4
UF	95±9	95±9	93±9
QU	100±0	98±1	85±5
TN	100±0	98±1	80±8
CH	100±0	100±0	95±1
LF	100±0	98±1	81±7

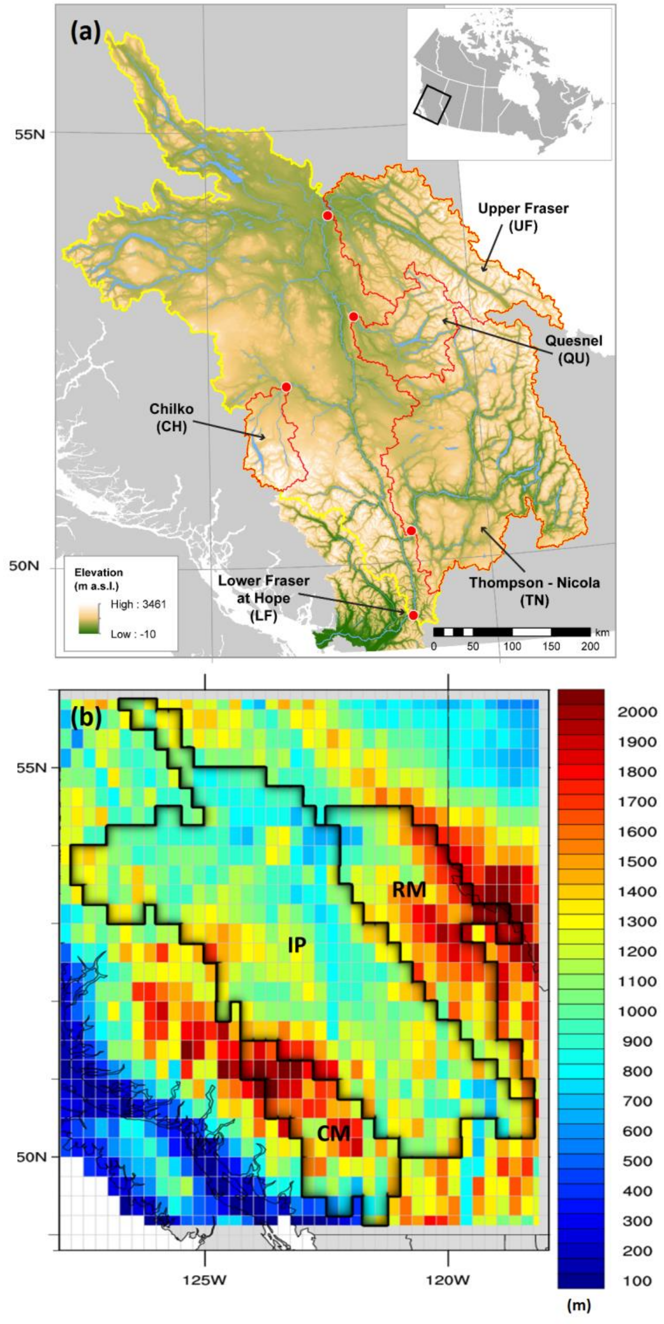

Figure 1: (a) Digital elevation map of the FRB with identification of sub-basins: Upper Fraser (UF), Quesnel (QU), Chilko (CH), Thompson–Nicola (TN), and Fraser at Hope (LF). (b) Elevation map highlighting the Fraser River Basin and three geoclimatic regions. RM, IP and CM represent the Rocky Mountains, Interior Plateau and Coast Mountains, respectively. Elevations are in meters and the horizontal grid resolution is that of the VIC hydrological model (0.25°).

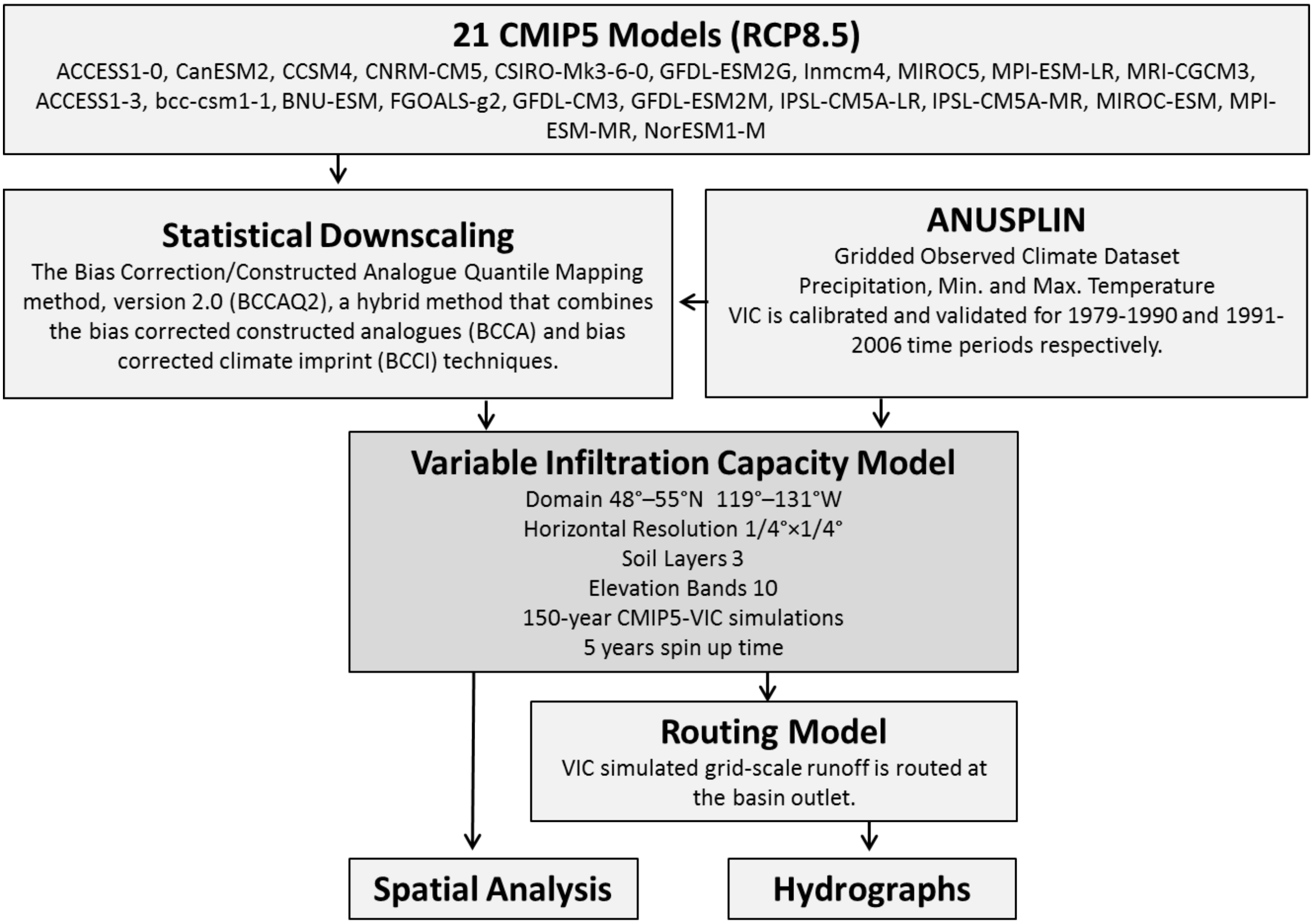

Figure 2: Block diagram of the VIC model experimental setup and analysis.

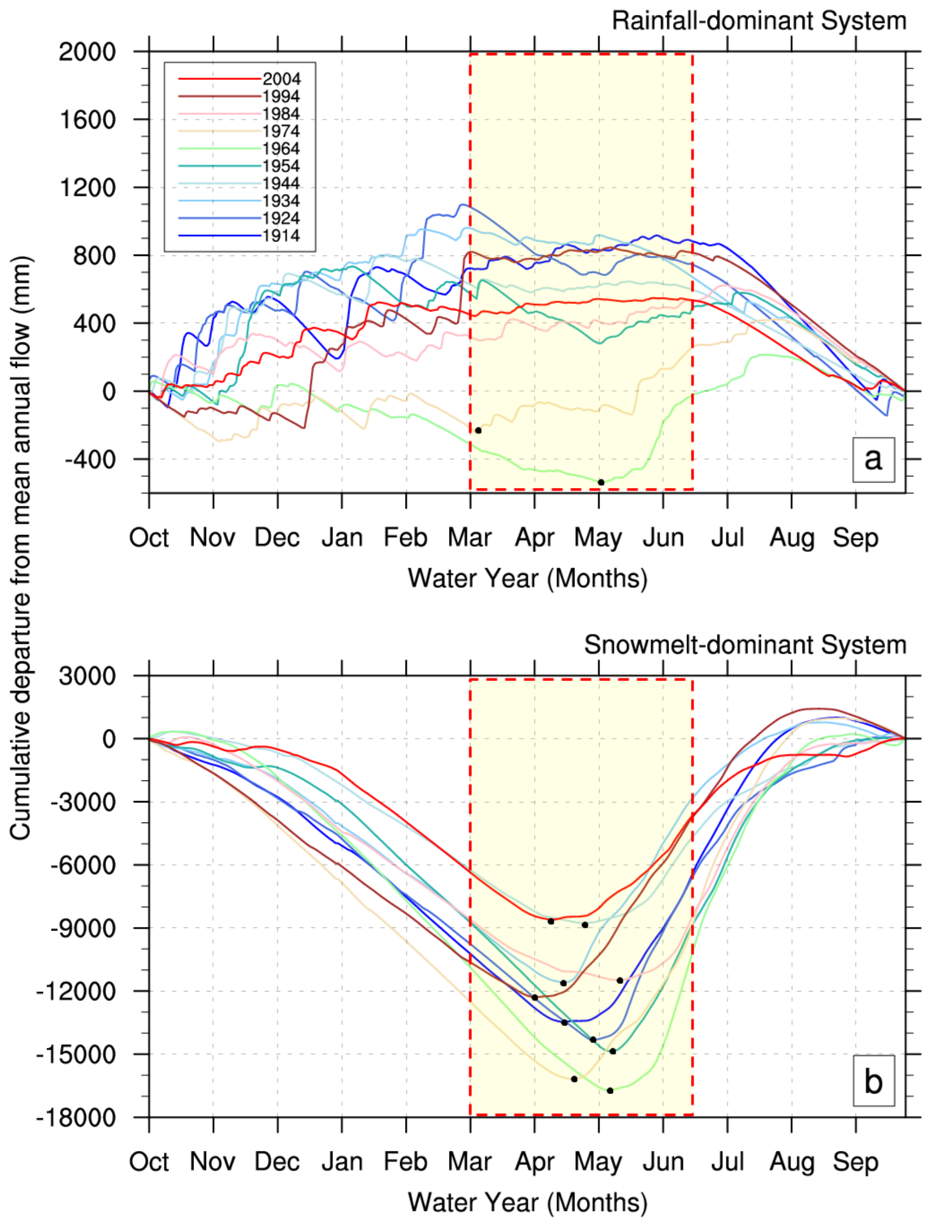

Figure 3: Cumulative departure from the water year's mean observed flow for the (a) Capilano River Above Intake (WSC ID 08GA010) and (b) Fraser River at Hope (WSC ID 08MF005), for 10 years within the 1914-2010 time period. Panel (a) demonstrates a rainfall-dominant system where snowmelt pulses (SPs) are detected in only two of the ten years whereas panel (b) illustrates a river where there are clear SPs in all the selected years. Black dots represent the day of water year (i.e. SP) when cumulative departure from the mean flow is a water year maximum.

Hydrol. Earth Syst. Sci. Discuss., https://doi.org/10.5194/hess-2018-232
Manuscript under review for journal Hydrol. Earth Syst. Sci.
Discussion started: 14 May 2018

Hydrology and Earth System Sciences
Open Access
Discussions

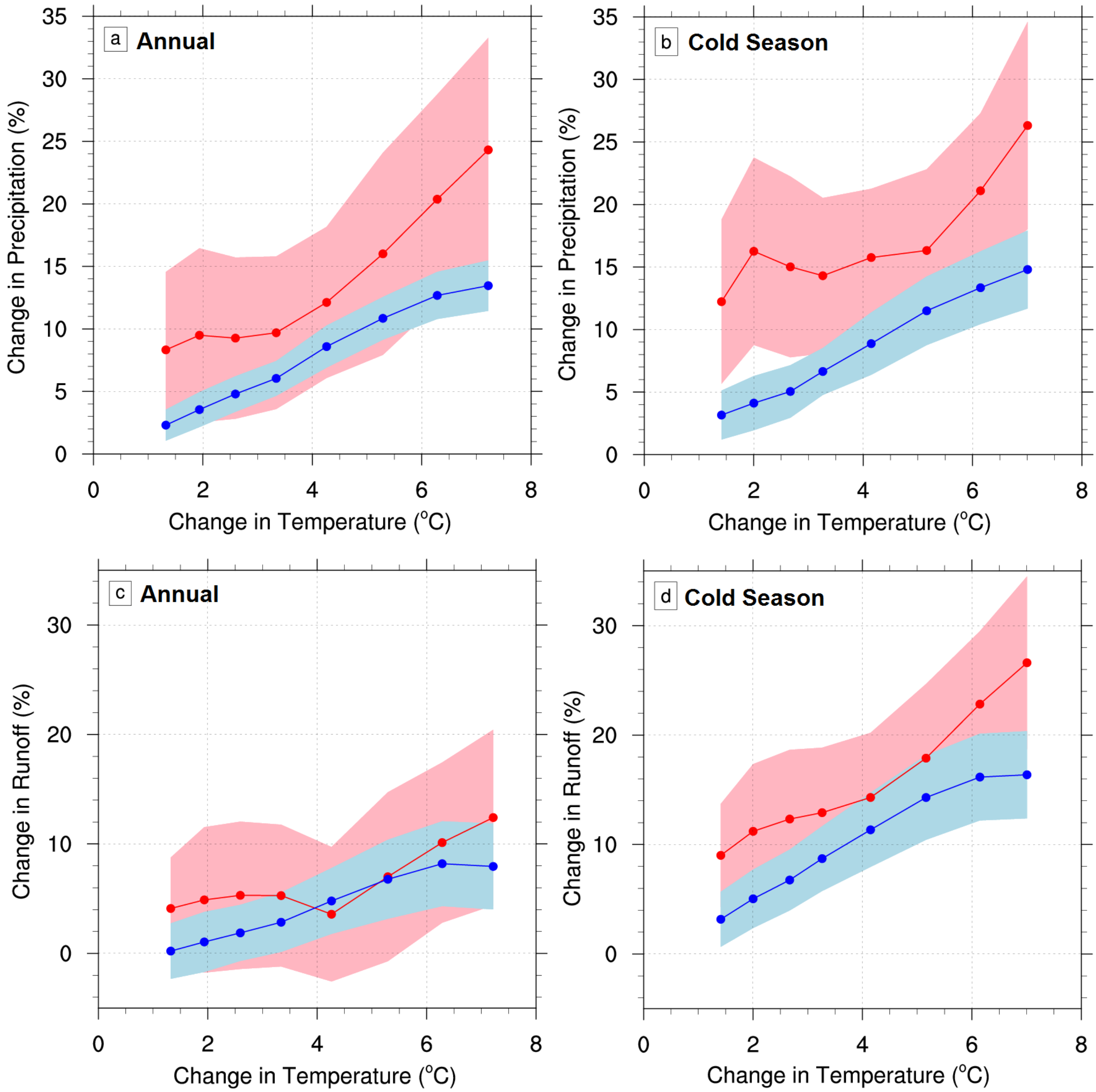

Figure 4: Rate of change of mean and interannual variability with warming for (a, b) precipitation and (c, d) runoff. Change in mean (blue line) and interannual standard deviation (red line) are averaged over the FRB and are shown as a function of FRB mean temperature change. Each marker indicates a 30-year period centred on consecutive decades between 2010 and 2099 relative to the 1990s base period. Shading represents inter-model spread as indicated by a 5-95% confidence interval.

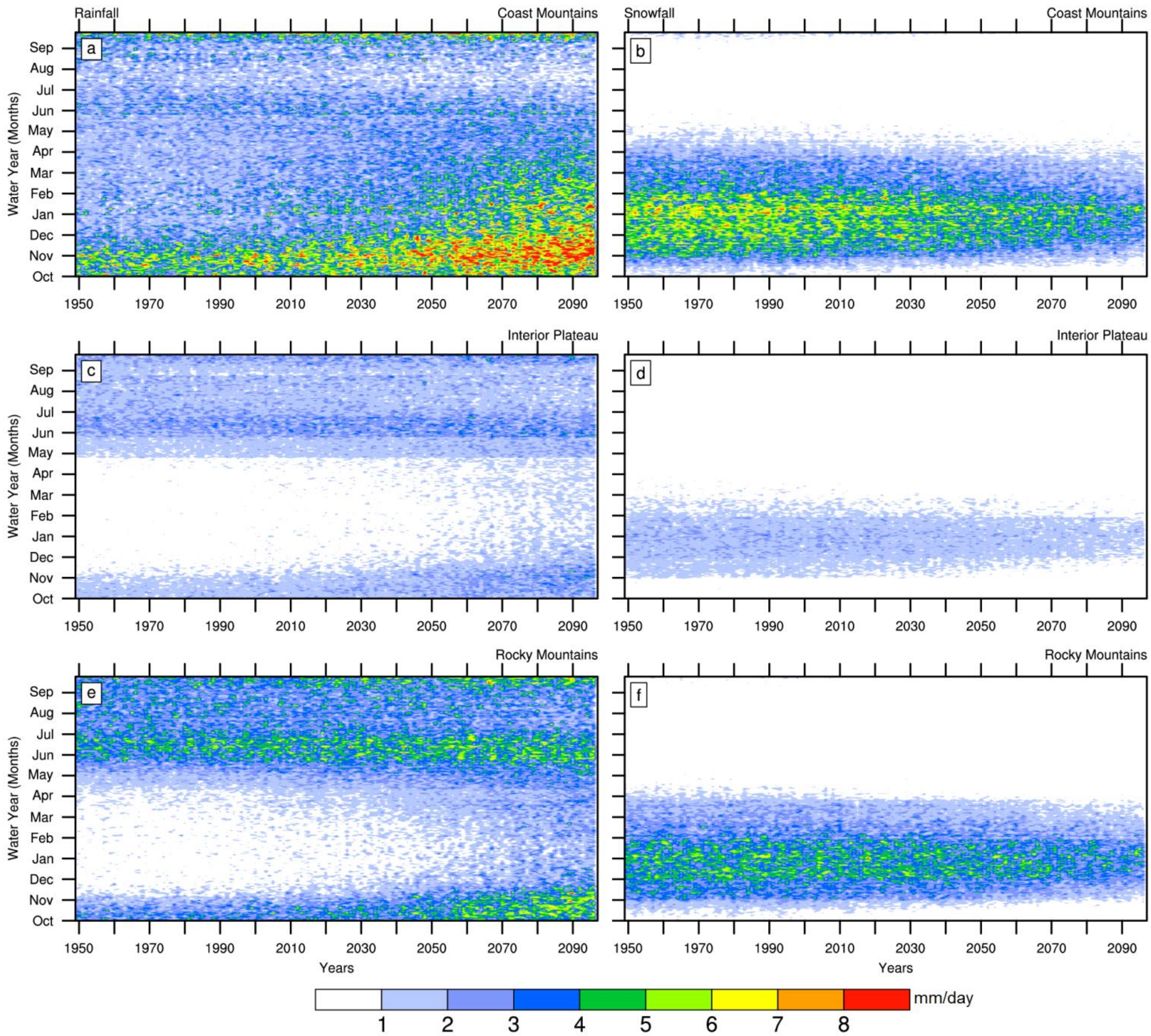

Figure 5: Partitioning of CMIP5 models MME mean total precipitation (mm day^{-1}) into daily (a, c, e) rainfall and (b, d, f) snowfall for the (a, b) Coast Mountains, (c, d) Interior Plateau and (e, f) Rocky Mountains. Values are regional spatial averages over the three geoclimatically defined regions. Units are in mm day^{-1}.

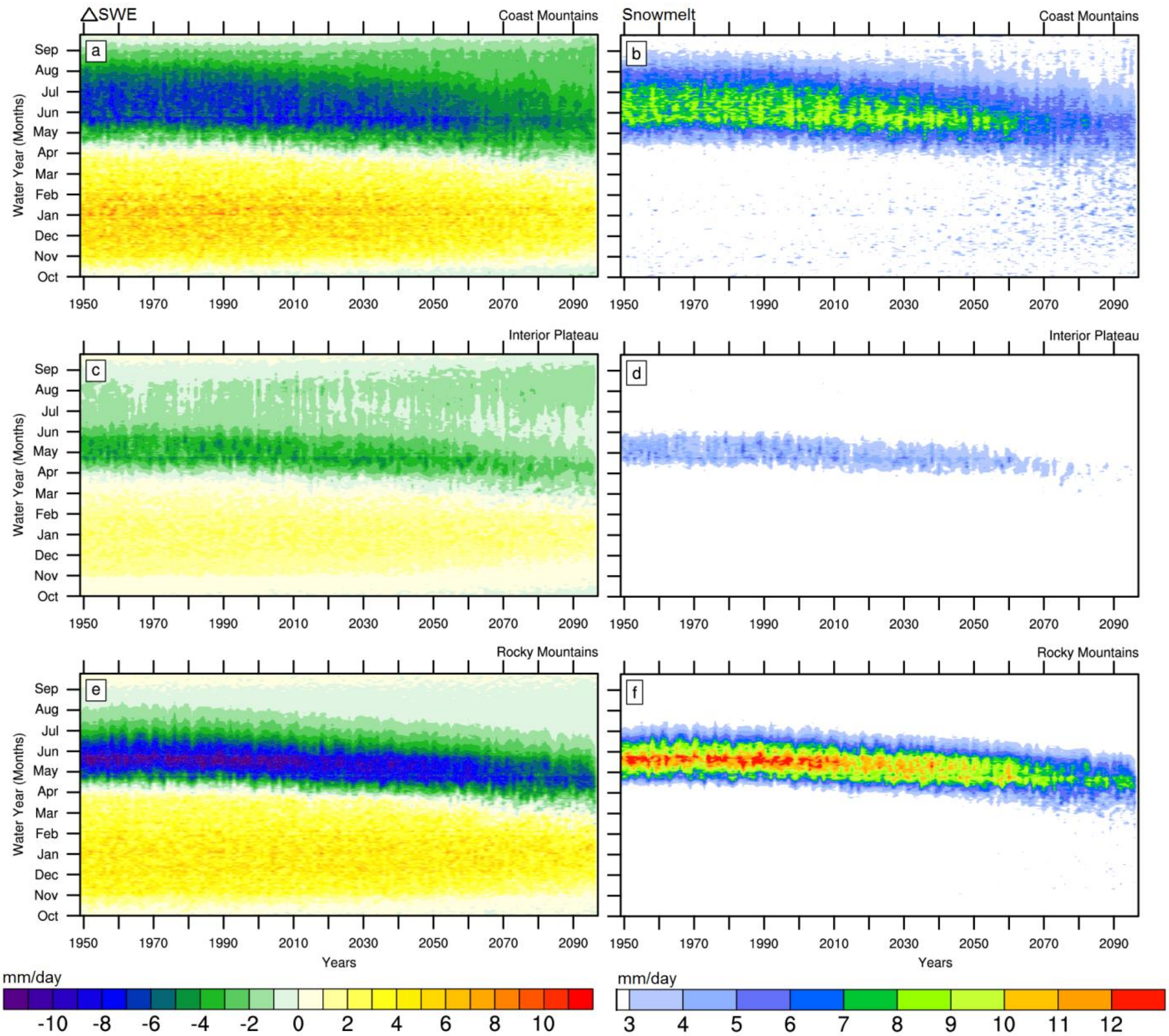

Figure 6: CMIP5-VIC simulated MME mean (a, c, e) ΔSWE (daily SWE rate) and (b, d, f) snowmelt for the (a, b) Coast Mountains, (c, d) Interior Plateau and (e, f) Rocky Mountains. In panels (a), (c) and (e), values greater than 0 represent snow accumulation and those below 0 are snow ablation. Units are in mm day^{-1}.

Hydrol. Earth Syst. Sci. Discuss., https://doi.org/10.5194/hess-2018-232
Manuscript under review for journal Hydrol. Earth Syst. Sci.
Discussion started: 14 May 2018

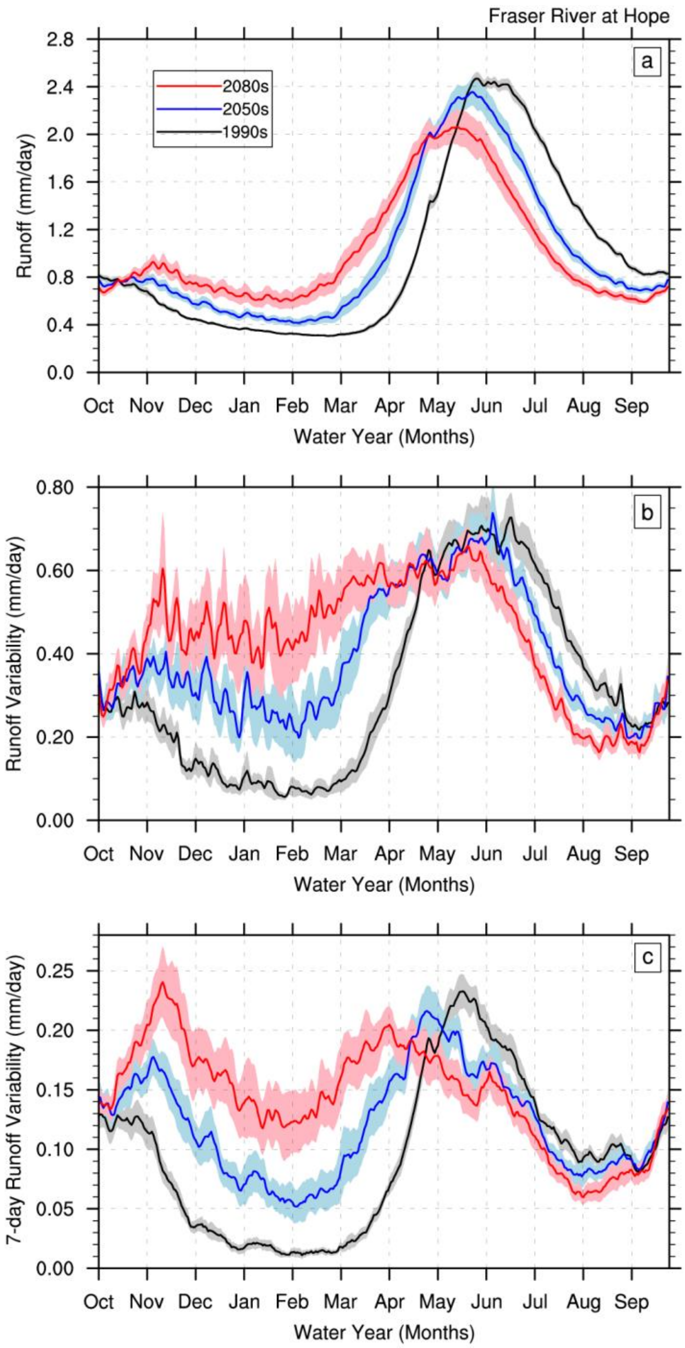

Figure 7: CMIP5-VIC simulated daily runoff (a) mean, (b) variability and (c) 7-day variability for the Fraser River at Hope. Black, blue and red curves represent the MME mean for the 1990s, 2050s and 2080s, respectively. Shading represents inter-model spread as indicated by a 5-95% confidence interval.

Hydrol. Earth Syst. Sci. Discuss., https://doi.org/10.5194/hess-2018-232
Manuscript under review for journal Hydrol. Earth Syst. Sci.
Discussion started: 14 May 2018

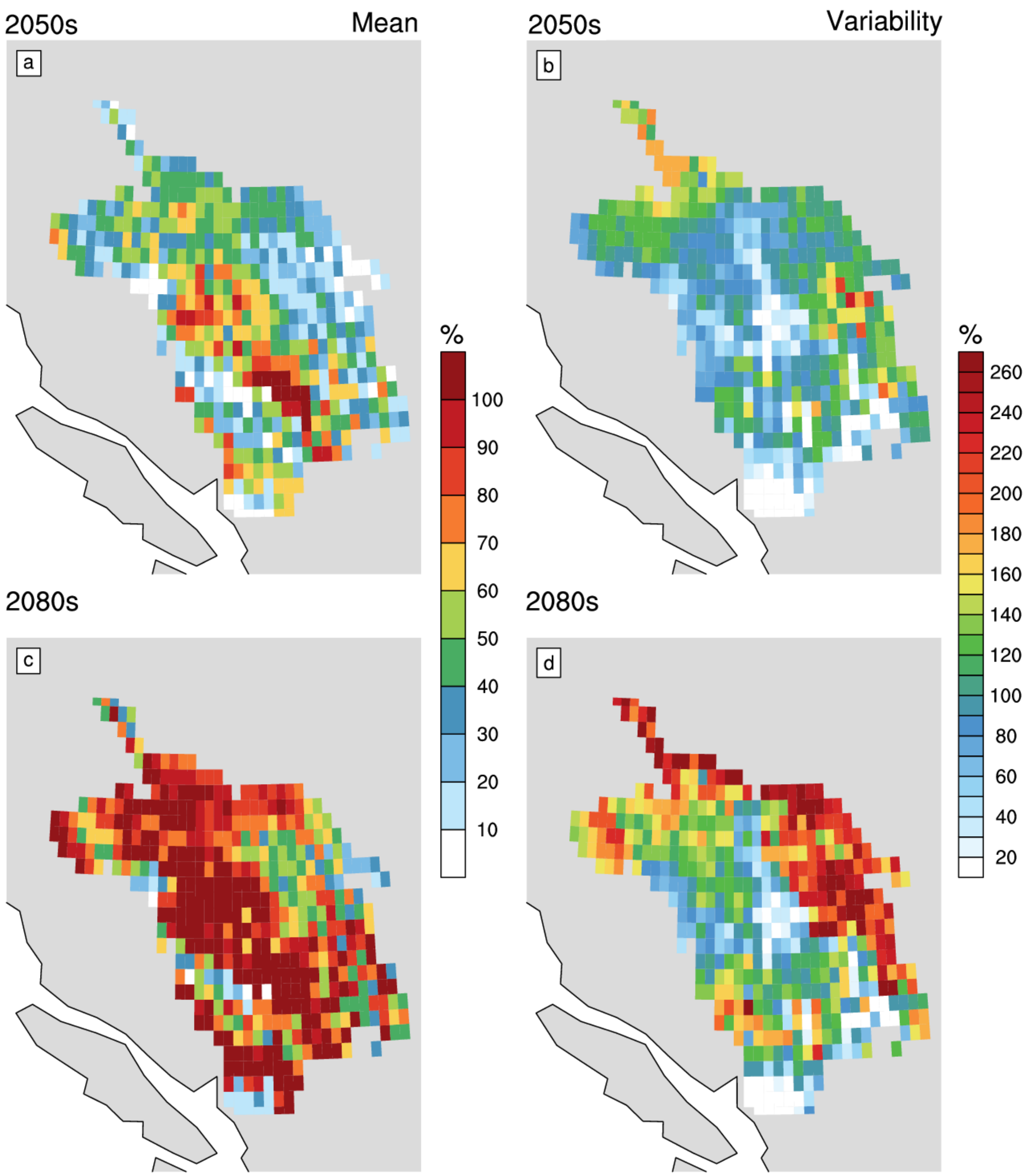

Figure 8: Spatial patterns of change (%) in MME (a, c) mean and (b, d) interannual variability of CMIP5-VIC simulated cold season runoff in the 2050s and 2080s relative to the 1990s.

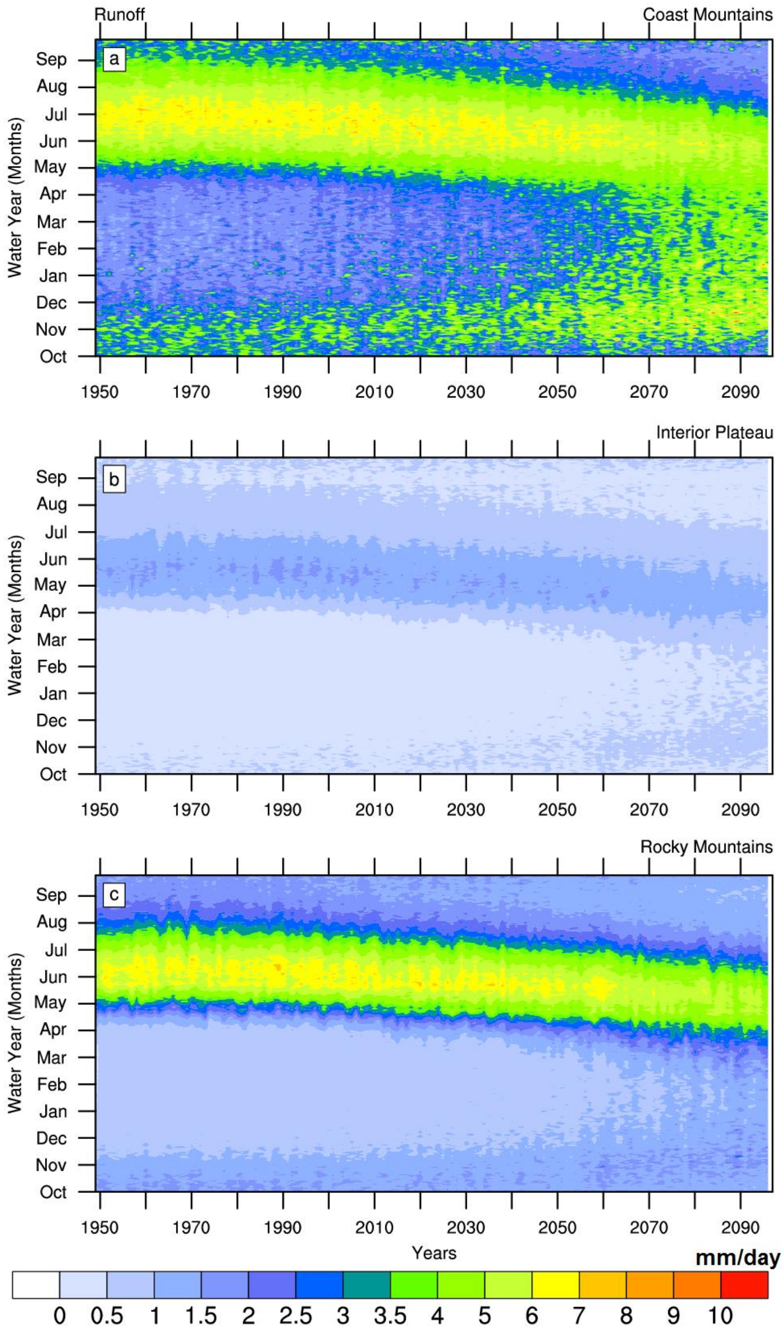

Figure 9: CMIP5-VIC simulated mean daily runoff (mm day^{-1}) for Coast Mountains, Interior Plateau and Rocky Mountains. Values are spatial averages over regional gridcells.

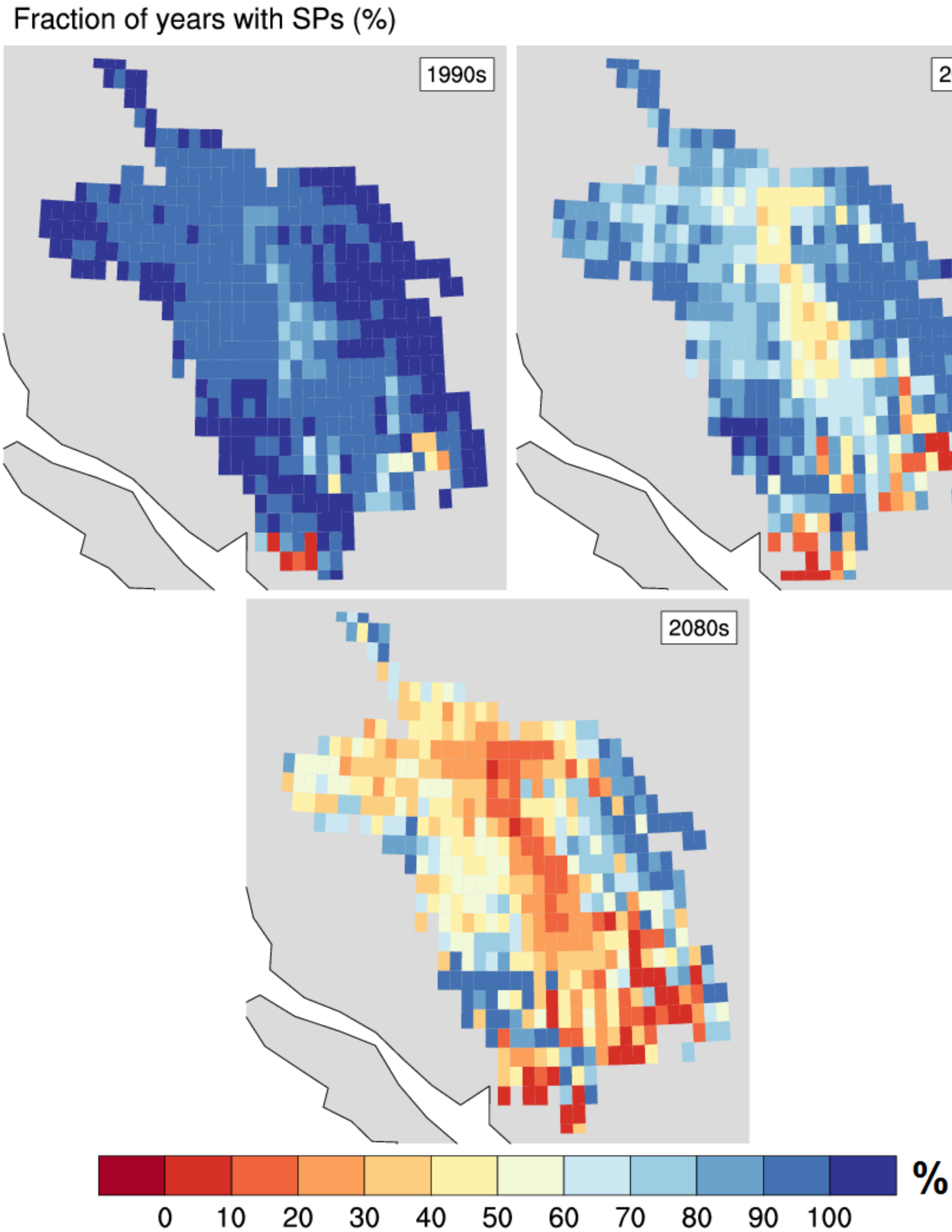

Figure 10: CMIP5-VIC simulated MME mean fraction of years with snowmelt pulses (SP, %) in the (a) 1990s, (b) 2050s, and (c) 2080s. Zero values are assigned to gridcells where no snowmelt pulses are detected.

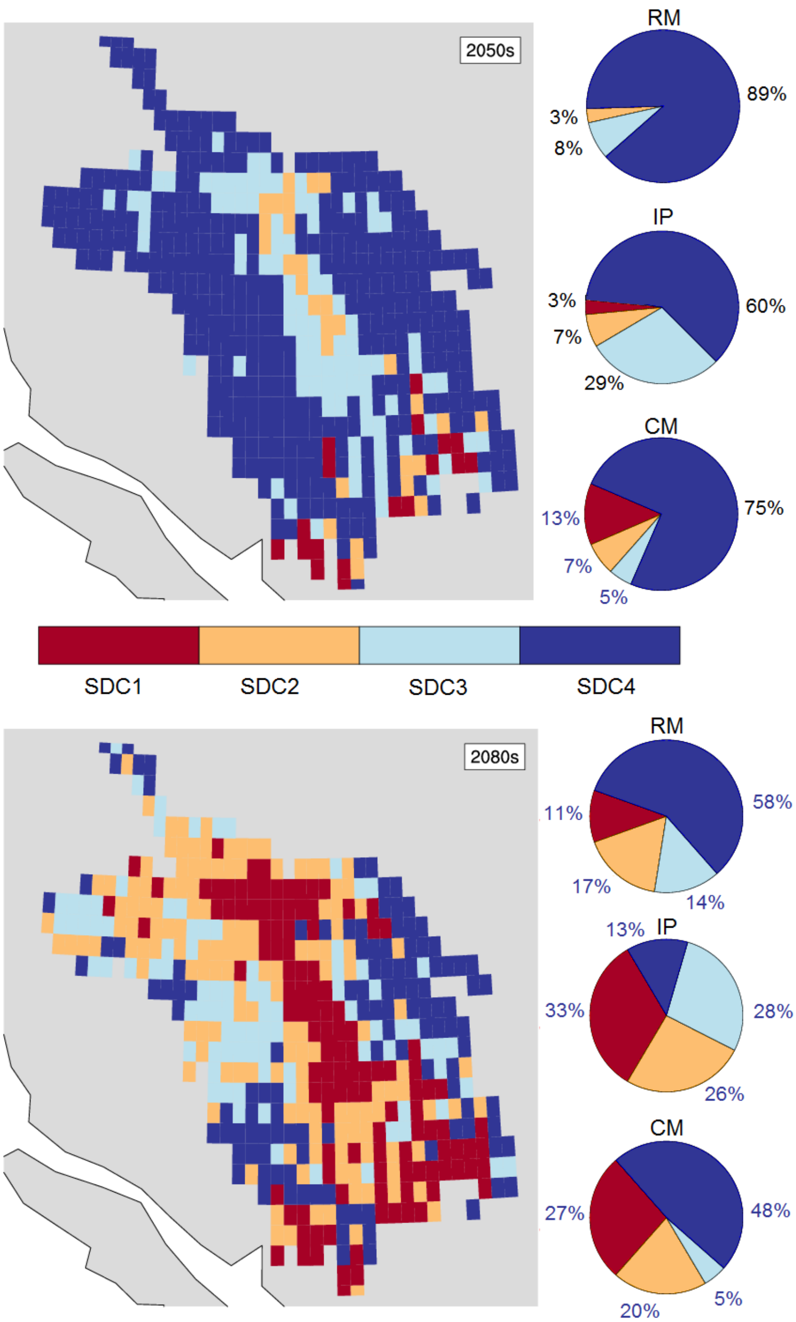

Figure 11: CMIP5-VIC simulated MME mean projected Snowmelt-dominant Categories (SDC) in the 2050s and 2080s relative to 1990s. SDCs are classified using the SP detection algorithm and are based on changes (%) in the fraction of years with SP (see Sec. 2.5 for details). Pie charts show corresponding change in fraction of gridcells (%) in the Rocky Mountains (RM), Interior Plateau (IP) and Coast Mountains (CM) geoclimatic regions.